Electro-optic switching element for dielectric-loaded surface plasmon polariton waveguides

A. V. Krasavin[a] and A. V. Zayats
Centre for Nanostructured Media, IRCEP, The Queen's University of Belfast, Belfast BT7 1NN, United Kingdom

(Received 25 April 2010; accepted 25 June 2010; published online 27 July 2010)

We present three-dimensional numerical modeling of an active electronically controlled switching element for fully-functional plasmonic circuits based on dielectric-loaded surface plasmon polariton waveguides. It has been demonstrated that the transmission of the guided mode through a highly wavelength-selective waveguide ring resonator (WRR) can be efficiently controlled with very small refractive index changes of the order of 10^{-3}, achievable through the electro-optic effect in nonlinear materials. Furthermore, we have introduced a figure of merit for such active plasmonic elements and optimized the active WRR performance in terms of its sensitivity and size. These results shows the potential to create high performance 600 nm radius plasmonic WRR switches. © *2010 American Institute of Physics*.
[doi:10.1063/1.3464552]

Dielectric-loaded surface plasmon polariton waveguides (DLSPPWs) have proved to be an efficient means to localize and guide photonic signals in a form of SPP waves. SPPs are electromagnetic excitations coupled to free electron oscillations propagating in a wave-like fashion along a flat dielectric-metal interface or a waveguide.[1] DLSPPWs are produced by a dielectric (e.g., polymer) stripe placed on a metal surface [Fig. 1(a)]. Two-dimensional eigenmode numerical simulations show that at the telecom wavelength a 600×600 nm^2 polymer/gold DLSPP waveguide is single-mode for SPP waves, supporting only a fundamental transverse magnetic (TM_{00}) SPP mode. Recently, an exhaustive variety of efficient DLSPPW passive elements have been demonstrated both theoretically and experimentally.[3–9] DLSPPWs are extremely robust to fabricate using a standard photo- or electron beam lithography,[4] nanoimprint,[7] or two-photon polymerization.[8] However, to construct a fully-functional circuitry able not only to guide but also to process photonic signals, active components should be introduced.[5,10,11] Here, using full three-dimensional (3D) numerical modeling we demonstrate a compact and efficient SPP switch based on a waveguide ring resonator (WRR) and controlled by an external voltage through the electro-optic effect. Its performance may lead to the realization of fully-functional plasmonic circuitry for hybrid information processing devices, which combines both electronic and optical components.

A distinct advantage of DLSPPWs among other types of waveguides is that the dielectric core of the waveguide can be easily functionalized to be an active medium. Exploiting this, we propose an active plasmonic component on the basis of a WRR (Fig. 1), which has been shown to possess strong wavelength selectivity, and therefore, sharp resonant transmission features.[6] To this end, the transmission of an SPP signal through the WRR (from port *A* to port *B*) is defined by interference between the SPP mode passed along the straight section and the mode coupled to the ring. Using an electro-optic polymer for the waveguides and an electrode on top of the ring allows the effective refractive index of the ring mode to be controlled by an external voltage. Thus, the phase shift, and therefore, interference will be controlled modulating the SPP transmission through the WRR. In order to take advantage of the electro-optic effect, the polymer should be poled. This can be done using the same control electrode.

Despite small SPP field near the top surface of the waveguide [Fig. 1(a)], the mode pattern is completely changed when the metal electrode at the top is introduced. The plasmonic modes on the top and the bottom metal-polymer interfaces are no longer degenerated, producing two waveguide modes with symmetric and antisymmetric distributions of the vertical component of the electric field [Fig. 1(c)]. For a 600×600 nm^2 waveguide cross-section, in the telecom wavelength range, the antisymmetric mode is very close to

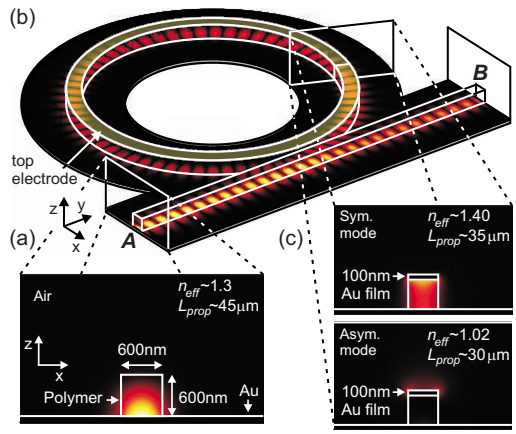

FIG. 1. (Color online) (a) Cross-section of 600×600 nm^2 polymer ($n_1=1.493$)/gold [$n_2=0.55-11.5i$ at $\lambda=1550$ nm (Ref. 2)] DLSPP waveguide and $|E_z|$ field profile of a fundamental TM_{00} SPP mode. (b) Active element based on a waveguide ring resonator: a waveguide ring made from electro-optic polymer placed in the vicinity of the main waveguide, which enables coupling to the ring SPP mode. A 100 nm thick metal electrode is placed on the top of the ring to control the WRR transmission from the input port *A* to the output port *B*. The field map shows $|\mathrm{Re}(E_z)|$ cross-section 10 nm above the bottom metal interface. (c) Field profiles of symmetric and antisymmetric modes appearing when the metal electrode is placed on the waveguide.

[a]Electronic mail: a.krasavin@qub.ac.uk.

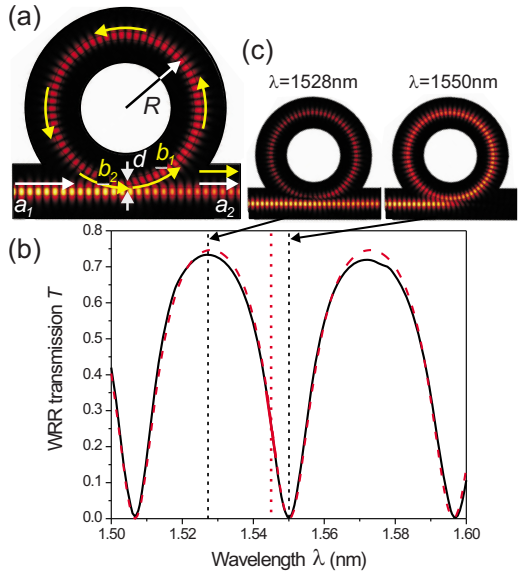

FIG. 2. (Color online) (a) $|\mathrm{Re}(E_z)|$ cross-section of the fields in the WRR, taken 10 nm above the bottom metal surface. The arrow sketch shows the redistribution of the power flow and interference of the modes in the WRR output. (b) Transmission of the WRR as a function of the wavelength: solid black curve represents numerical simulation results, dashed red curve represents the analytical fit using Eq. (1). Red dotted line marks the wavelength $\lambda=1545$ nm with the highest gradient of the WRR transmission. (c) Field maps corresponding to the maximum and the minimum transmission at $\lambda=1528$ nm and $\lambda=1550$ nm, respectively. The radius of the ring and the gap between the ring and the straight waveguide are adjusted to be $R=5.436$ μm and $d=128$ nm.

the cut-off ($n_{\mathrm{eff}}\sim 1.02$), and its field is essentially pushed out of the gap between the ring and the waveguide. Thus, it can be expected that while passing the region adjacent to the ring the main DLSPPW mode should be mainly coupled to the symmetric mode. Performing full 3D numerical simulations, it was confirmed that the coupling process is very efficient with negligible scattering in the coupling region.

The performance of the WRR can be briefly explained in the following way. The incident SPP mode passing through the waveguide region adjacent to the ring is partly coupled to the mode in the ring [Fig. 2(a)]. The latter starts to circulate around the ring, after each cycle being partly decoupled into the WRR output.[12] There it interferes with the mode in the straight waveguide which passed through the coupling region. The result of interference is defined by a phase delay acquired by the ring mode or, in other words, by the number of mode wavelengths $\lambda/n_{\mathrm{eff}}^{\mathrm{ring}}$ along the optical path of the ring. Thus, at a fixed ring radius while scanning through the wavelengths, the oscillations between minimum and maximum WRR transmission are observed, with sharp resonances in the minimum transmission [Figs. 2(b) and 2(c)]. The particular wavelengths at which the minima occurs are determined by the ring radius and the mode effective refractive index. The ring radius $R=5.436$ μm was adjusted so that the minimum transmission is at the telecom wavelength region $\lambda=1550$ nm. On the other hand, the gap distance d defines partial amplitudes with which the mode is divided in the coupling region and eventually interfere, thus being responsible for the transmission modulation contrast. This distance was optimized to be 128 nm so that the transmission in the minima is zero. This way, sharp resonances and, therefore, steepest slopes in the transmission spectrum have been achieved, where small changes in wavelength lead to dramatic changes in the transmission.

The comb-like shape of the transmission through the WRR element can be described by a formula, based on the interference model, as follows:[12,13]

$$T(\alpha,t,\theta)=\frac{\alpha^2+t^2-2\alpha t\cos(\theta)}{1+\alpha^2t^2-2\alpha t\cos(\theta)}, \tag{1}$$

where

$$\theta=\frac{2\pi}{\lambda}n_{\mathrm{eff}}\times 2\pi R+\phi \tag{2}$$

is the phase shift acquired by the mode traveling a complete circle around the ring. Here, t is the amplitude transmission coefficient ($a_2=te^{i\psi}a_1$) for the mode in the straight waveguide and α is the amplitude loss coefficient of the ring ($b_2=b_1\alpha e^{i\theta}$), as shown in Fig. 2(a). The additional phase ϕ is the coupling-induced phase shift[13] which takes into account shift of the resonance of the isolated waveguide ring due to the presence of the main waveguide coupled to it. We estimated its value by increasing the gap d to the range where the ring is practically isolated and monitoring the change in the minimum transmission wavelength. These simulations gave us also an opportunity to precisely estimate the effective refractive index of the ring mode in the working spectral range $\mathrm{Re}(n_{\mathrm{eff}}^{\mathrm{ring}})=1.579-0.112\times\lambda[\mu\mathrm{m}]$. The values of $n_{\mathrm{eff}}^{\mathrm{ring}}$ are very close to 1.4, corresponding to the effective refractive index of the symmetric mode [Fig. 1(c)]. The analytical model describes the numerical results extremely well [Fig. 2(b)]. From fitting the obtained results with analytical dependence given by Eq. (1), we can find the intrinsic parameters of the WRR $\alpha\sim 0.59$ and $t\sim 0.56$. The obtained energy loss in the ring $\alpha^2\sim 0.35$ is in agreement with the value of $\alpha^2=0.34$, obtained from the simulations of the bent waveguide with the control electrode.

The performance of the WRR in response to an electronic control signal has been numerically studied. The crucial parameter here is sensitivity of the WRR transmission to the change in the refractive index of the ring material induced through the electro-optic effect. For the best WRR performance it is logical to use the wavelength at which the phase changes play the most dramatic role, that is the one in the region of the steepest slope at the WRR wavelength characteristics, e.g. $\lambda=1545$ nm [red dotted line in Fig. 2(b)]. We found that the changes of WRR transmission can be very strong for realistic changes of the refractive index (Fig. 3). The refractive index modulation of $\pm 2\times 10^{-3}$ leads the changes in WRR transmission by almost three times. The modulation contrast is as high as $(T_{\max}-T_{\min})/(T_{\max}+T_{\min})\sim 0.5$. Moreover, the crucial advantage of the proposed device is that the required changes in the refractive index are realistic with the Pockels electro-optic coefficients in nonlinear polymers (~ 170 pm/V) which have already been observed.[14]

The performance of the active WRR was further optimized varying the ring radius and introducing a figure of merit (FOM) $M=(\partial T/\partial n)/(R/\lambda)$. The FOM determines the ratio between device sensitivity to the control refractive index change and its size, normalized to the wavelength. The nominator of FOM can be expanded as $\partial T/\partial n=(\partial T/\partial\theta)\times(\partial\theta/\partial n_{\mathrm{eff}})(\partial n_{\mathrm{eff}}/\partial n)$. The first derivative here was calcu-

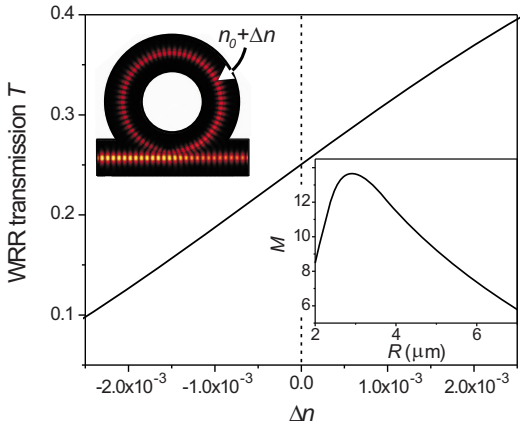

FIG. 3. (Color online) Active WRR element (top inset): the dependence of the WRR transmission on the change in the refractive index of the electro-optic material. The bottom inset shows the dependence of the FOM M on the ring radius.

lated using Eq. (1), which analytically determines the SPP transmission through the WRR. A given value of radius R corresponds to a certain value of the round-trip losses α, which was estimated by modeling waveguide bends. Then for each fixed R (or α) taking derivatives of T over θ and t in Eq. (1), we found the maximum of the transmission sensitivity to the round-trip phase shift ($\partial T/\partial\theta$) and further optimized it in terms of t (or, in other words, the waveguide-ring separation d). The middle derivative in the expanded expression was calculated using Eq. (2) and the last derivative was estimated using waveguide-with-electrode eigenmode simulations. Finally, the FOM for the case of WRR was calculated as

$$M = \frac{\partial T/\partial n}{R/\lambda} = 4\pi^2 \frac{\partial T}{\partial \theta}\frac{\partial n_{\mathrm{eff}}}{\partial n}. \tag{3}$$

Here, $\partial T/\partial\theta$ is determined by the geometrical parameters of the structure, while $\partial n_{\mathrm{eff}}/\partial n$ carries the information on the nature of the control process (nonlinear-optical, thermo-optical, or electro-optical, etc.) and the field distribution in the waveguide. For example, for plasmonic waveguides it takes into account the localization of the field near the metal, the field enhancement effects and possible slow-light effects.

The resulting dependence of the FOM on the ring radius is presented in the inset to Fig. 3. One can see that the performance of the active WRR element can be even further improved by the factor of $\sim$1.7 via implementing the rings with just 3 μm radius. Moreover, FOM shows that it is beneficial to use high-refractive index nonlinear materials, such as barium titanate. In this case for a 300×300 nm^2 waveguide, the ring radius can be as small as $\sim$0.6 μm, and the FOM of the WRR can reach almost 30.

In conclusion, using numerical simulations we have demonstrated a highly compact and efficient electronically controlled active plasmonic element on the basis of the waveguide ring resonator. The plasmonic signal transmission through the WRR can be modulated with high contrast through the electro-optic effect with the refractive index change in the order of 10^{-3}, presently achievable with nonlinear polymers. Finally, by introducing a FOM for such active plasmonic components, the performance of the active WRR element was optimized in terms of its sensitivity and size. This clearly shows the potential to create high performance 600 nm radius plasmonic WRRs based on $BaTiO_3$. The proposed FOM is a universal measure which can be used for the comparison of active elements based on dielectric or plasmonic waveguides regardless of the type of control signal used to change the mode effective index.

This work was supported in part by EPSRC (UK) and EC FP6 STREP PLASMOCOM. The authors acknowledge the fruitful discussions with S. I. Bozhevolnyi and W. Dickson.

[1]H. Raether, *Surface Plasmons on Smooth and Rough Surfaces and Gratings* (Springer, New York, 1988).
[2]*Handbook of Optical Constants of Solids*, edited by E. D. Palik (Academic, New York, 1984).
[3]I. I. Smolyaninov, Y.-J. Hung, and C. C. Davis, Appl. Phys. Lett. **87**, 241106 (2005).
[4]T. Holmgaard, Z. Chen, S. Bozhevolnyi, L. Markey, A. Dereux, A. Krasavin, and A. Zayats, Opt. Express **16**, 13585 (2008).
[5]J. Gosciniak, S. I. Bozhevolnyi, T. B. Andersen, V. S. Volkov, J. Kjelstrup-Hansen, L. Markey, and A. Dereux, Opt. Express **18**, 1207 (2010).
[6]T. Holmgaard, Z. Chen, S. I. Bozhevolnyi, L. Markey, A. Dereux, A. V. Krasavin, and A. V. Zayats, Appl. Phys. Lett. **94**, 051111 (2009); Z. Chen, T. Holmgaard, S. I. Bozhevolnyi, A. V. Krasavin, A. V. Zayats, L. Markey, and A. Dereux, Opt. Lett. **34**, 310 (2009).
[7]A. Seidel, C. Ohrt, S. Passinger, C. Reinhardt, R. Kiyan, and B. N. Chichkov, J. Opt. Soc. Am. B **26**, 810 (2009).
[8]C. Reinhardt, A. Seidel, A. B. Evlyukhin, W. Cheng, and B. N. Chichkov, J. Opt. Soc. Am. B **26**, B55 (2009).
[9]A. V. Krasavin and A. V. Zayats, Phys. Rev. B **78**, 045425 (2008); Opt. Express **18**, 11791 (2010).
[10]A. V. Krasavin and N. I. Zheludev, Appl. Phys. Lett. **84**, 1416 (2004).
[11]K. F. MacDonald, Z. L. Samson, M. I. Stockman, and N. I. Zheludev, Nature Photon. **3**, 55 (2009).
[12]A. Yariv and P. Yeh, *Photonics: Optical Electronics in Modern Communications* (Oxford University Press, Oxford, 2007).
[13]M. A. Popovic, C. Manolatou, and M. R. Watts, Opt. Express **14**, 1208 (2006).
[14]Y. Enami, C. T. Derose, D. Mathine, C. Loychik, C. Greenlee, R. A. Norwood, T. D. Kim, J. Luo, Y. Tian, A. K.-Y. Jen, and N. Peyghambarian, Nature Photon. **1**, 180 (2007).